A New Model System for Lipid Interactions in Stratum Corneum Vesicles: Effects of Lipid Composition, Calcium, and pH†

Rita M. Hatfield‡,§ and Leslie W.-M. Fung*,‡

Department of Chemistry, Loyola University of Chicago, Chicago, Illinois 60626, and Helene Curtis, A Business Unit of Unilever Home and Personal Care-USA, Chicago, Illinois 60008

Received June 16, 1998; Revised Manuscript Received October 1, 1998

ABSTRACT: We prepared large unilamellar vesicles (LUVs) with three different stratum corneum lipid compositions: constant amounts of ceramides (55 wt %) and fatty acids (15%) with varying amounts of cholesterol sulfate (0−15%) and cholesterol (15−30%). One of the compositions served as a model for normal stratum corneum, while the second one served as a model for recessive X-linked ichthyosis stratum corneum. The third composition consisted of no cholesterol sulfate. Intervesicle lipid interactions in these LUVs were monitored by fluorescence methods for content leakage, and contents mixing at pH 9, in the absence and presence of Ca^{2+}, and at pH 6. Since the content leakage and contents mixing assays were originally developed for phospholipid vesicles, we characterized the probe binding and the probe quenching properties for stratum corneum LUV systems, and modified the assays slightly accordingly. The time-dependent fluorescence intensity changes in the probe-containing LUVs at pH 9 and 6 and in response to the addition of calcium were monitored. Our results demonstrated that all three types of LUVs were relatively stable at pH 9. Addition of Ca^{2+} or decreasing the pH to 6 activated intervesicle lipid mixing followed by vesicle fusion and lysis. We found that the LUVs with no cholesterol sulfate and 30% cholesterol exhibited a more extensive Ca^{2+}- or low-pH-activated intervesicle lipid interaction than LUVs with either 5% cholesterol sulfate and 25% cholesterol or 15% cholesterol sulfate and 15% cholesterol. These results suggest that fusogenic agents such as Ca^{2+} and H^+ act to neutralize the fatty acids in the lipid bilayer of stratum corneum vesicles. The inclusion of 5−15% cholesterol sulfate helps to prevent the collapse of fused vesicles into other structures.

The stratum corneum layer of the skin, which forms a barrier between the skin and the external environment, is composed of corneocytes (dead cells) in a lipid matrix. The lipids, with ceramides as the main component and with little phospholipids (*1*, *2*), are assembled in lamellar sheets (*3*, *4*). The lipid composition of the stratum corneum can affect desquamation, the processes involved in the detachment and subsequent removal of corneocytes at the skin surface, resulting in disorders of cornification (*5*, *6*). Stratum corneum lipid abnormalities have been reported in inherited disorders such as ichthyosis and in common scaling disorders such as psoriasis and atopic dermatitis (*6*). Recessive X-linked ichthyosis patients lack steroid sulfatase (*7*, *8*), resulting in accumulation of cholesterol sulfate and decreased cholesterol levels in the stratum corneum (*9*, *10*). Consequently, prolonged stratum corneum retention (*10*) and thus excessive scaling of the skin occur. The molecular mechanism by which cholesterol sulfate affects stratum corneum shedding is not clear. It appears that the degree of scaling in patients suffering from X-linked ichthyosis can be reduced by cholesterol replacement therapy (*11*, *12*). A topical application of unilamellar vesicles/liposomes with the appropriate lipid composition may potentially change the cholesterol sulfate:cholesterol ratio in the stratum corneum by removing excess cholesterol sulfate as well as by inserting exogenous cholesterol (*11*). In addition, the topical application of physiological lipids with cholesterol as the dominant lipid in a propylene glycol/*n*-propanol vesicle was found to accelerate barrier recovery in chronically aged murine epidermis and human skin (*13*). The effects of Ca^{2+} and H^+ on intervesicle lipid interactions containing altered cholesterol sulfate:cholesterol ratios to reflect normal and ichthyosis lipid compositions have not been studied in detail. Information on lipid interactions as a function of the cholesterol/cholesterol sulfate composition may shed light on the behavior of these sterol molecules in the maintenance of the stratum corneum barrier in vivo.

We have demonstrated that large unilamellar vesicles (LUVs)[1] with 5% cholesterol sulfate and 25% cholesterol, together with 55% ceramides and 15% fatty acids, are stable

† Supported by Loyola University of Chicago and Helene Curtis, A Business Unit of Unilever Home and Personal Care-USA.

‡ Loyola University of Chicago.

§ Helene Curtis, A Business Unit of Unilever Home and Personal Care-USA.

[1] Abbreviations: ANTS, 8-aminonaphthalene-1,3,6-trisulfonic acid, disodium salt; DPPC, dipalmitoylphosphatidylcholine; DPX, *p*-xylene-bis-pyridinium bromide; I_t, fluorescence intensity measured at time *t*; I^T, total fluorescence intensity measured in the presence of 0.5% Triton X-100; LUVs, large unilamellar vesicles; LUV-N, LUV with 55% ceramides, 15% fatty acids, 5% cholesterol sulfate, and 25% cholesterol; LUV-X, LUV with 55% ceramides, 15% fatty acids, 15% cholesterol sulfate, and 15% cholesterol; LUV-Z, LUV with 55% ceramides, 15% fatty acids, no cholesterol sulfate, and 30% cholesterol; LUV^{xxx}, LUV encapsulated with xxx; MLVs, multilamellar vesicles; SUVs, small unilamellar vesicles.

10.1021/bi981421k CCC: $18.00
Published on Web 12/22/1998

at pH 9 and are good model systems for studying lipid properties of normal stratum corneum (*18*). The amount of cholesterol sulfate present in normal stratum corneum is smaller than that of cholesterol, but varies among different anatomical sites, with more cholesterol sulfate present in the leg (6.0%) and less in the abdomen (1.5%) or face (2.7%) (*15*). Additionally, various values, for example, 2.6% cholesterol sulfate and 15.6% cholesterol (*9*), 10% cholesterol sulfate and 25% cholesterol (*16*), or 5% cholesterol sulfate and 25% cholesterol (*2*, *17*), have been used to represent the lipid composition of normal stratum corneum. Some of the variations in the literature are, in part, due to the different lipid extraction techniques used. In recessive X-linked ichthyosis stratum corneum, the amount of cholesterol sulfate increases and the amount of cholesterol decreases. Williams and Elias reported values of 14.8% cholesterol sulfate and 9.0% cholesterol for recessive X-linked ichthyosis scale (*9*). Topical application of cholesterol sulfate to hairless mouse skin to double the amount of cholesterol sulfate in stratum corneum produced scale (*19*). In this work, we prepared LUVs with three different lipid compositions, all with constant amounts of ceramides (55%) and fatty acids (15%), but with differing ratios of cholesterol and cholesterol sulfate. The normal stratum corneum was represented by 5% cholesterol sulfate and 25% cholesterol (LUV-N), the recessive X-linked ichthyosis scale by 15% cholesterol sulfate and 15% cholesterol (LUV-X), and the third type by no cholesterol sulfate and 30% cholesterol (LUV-Z).

Intervesicle lipid interactions in these vesicles were monitored by fluorescence methods for content leakage and contents mixing. Since content leakage and contents mixing assays have been developed for phospholipid vesicles (*10*, *20*), and have not been used on nonphospholipid systems, we modified the published methods slightly for stratum corneum LUV systems. The modified assays were applied to systems at pH 9 in the absence and presence of Ca^{2+} and at pH 6. Our results demonstrated that Ca^{2+} and acidic pH affected intervesicle lipid−lipid interactions. Similar Ca^{2+} and H^+ effects were observed in LUVs representing both normal and ichthyosis lipid compositions, while different effects were observed in LUVs devoid of cholesterol sulfate.

EXPERIMENTAL PROCEDURES

Cholesterol, cholesterol sulfate, bovine brain ceramides types III and IV (containing α-hydroxy acids), lignoceric acid, octacosanoic acid, and dipalmitoylphosphatidylcholine (DPPC) were purchased from Sigma (St. Louis, MO), and palmitic acid was purchased from Fisher (Pittsburgh, PA). These chemicals were at least 99% pure and were used without further purification (*18*). 8-Aminonaphthalene-1,3,6-trisulfonic acid, disodium salt (ANTS), and *p*-xylene-bis-pyridinium bromide (DPX) were from Molecular Probes (Junction City, OR). Calcium chloride was from Spectrum (Gardena, CA). Other chemicals used to prepare buffers were purchased from Sigma, Fisher, or Calbiochem (La Jolla, CA). Borate buffer from Fisher (0.1 M boric acid/KCl/NaOH at pH 9) was used to prepare buffers used in the studies.

Preparations of LUVs with Different Lipid Compositions, with and without ANTS/DPX. Multilamellar vesicles (MLVs) (∼5 mg/mL) and extruded LUVs were prepared as described previously (*18*) with minor modifications. Since the addition of fluorescent probe ANTS and/or cationic quencher DPX to Fisher borate buffer increased the buffer osmolality, the osmolality of all samples was maintained at ∼270 mmol/kg, rather than at the previous value of ∼150 mmol/kg (*18*). ANTS or DPX solutions were prepared by dissolving chemicals in Fisher borate buffer. Since ANTS is acidic, it was necessary to add a small amount of NaOH to the solution to bring the pH back to 9.0. The osmolality of all solutions was adjusted to ∼270 mmol/kg with the addition of KCl. For example, 60, 52, 25, or 7 mM KCl was added to solutions without ANTS or DPX, with 25 mM ANTS, with 12.5 mM ANTS and 25 mM DPX, or with 50 mM DPX, respectively. The osmolality of buffers was checked by using a vapor pressure osmometer (Wescor, Inc., Logan, UT). These solutions were then added to lipid films to prepare MLVs containing different amounts of ANTS and DPX.

The MLVs were subjected to a repeated extrusion process until the sample absorbance at 700 nm was <0.250, to yield LUVs (*18*). Three types of lipid compositions were used to prepare three types of MLVs and subsequently three types of LUVs (LUV-N, LUV-X, and LUV-Z). All vesicles consisted of 55% (by weight) ceramides and 15% fatty acids. LUV-N also consisted of 5% cholesterol sulfate and 25% cholesterol to give a lipid composition similar to that in normal stratum corneum (*18*). LUV-X consisted of 15% cholesterol sulfate and 15% cholesterol to give a composition similar to that in recessive X-linked ichthyosis (*9*). LUV-Z consisted of no cholesterol sulfate, but 30% cholesterol. DPPC (100%) LUVs in Fisher borate buffer and 60 mM KCl were also prepared with extrusions at 48 °C through 0.4 and 0.1 μm filters.

The extruded samples were then loaded onto a Sephadex G-75 (Pharmacia, Piscataway, NJ) column with buffer containing 30 mM boric acid, 0.2 mM EDTA, and 140 mM KCl titrated to pH 9 with 1 N NaOH (osmolality of ∼270 mmol/kg) (borate column buffer) to give pure LUVs. The vesicle fractions were pooled and used as LUV samples at pH 9 for fluorescence measurements without further adjustment of lipid concentrations. The lipid concentrations of the final LUVs from different preparations ranged from 0.73 to 1.30 mg/mL and had an average value of 1.03 ± 0.35 mg/mL ($n = 24$). The concentrations of ANTS and DPX inside LUVs were not determined. The LUVs prepared with buffer solutions containing, for example, 25 mM ANTS, were designated as LUV^{25ANTS}. We prepared LUV-N^{25ANTS}, LUV-$N^{12.5ANTS/12.5DPX}$, LUV-$N^{12.5ANTS/25DPX}$, LUV-$N^{12.5ANTS/45DPX}$, and LUV-N^{50DPX}. Similar LUVs were prepared to yield probe-containing LUV-X and LUV-Z samples.

For samples with high DPX contents, frequent changes of membrane filters during repeated extrusion were necessary to keep the applied pressure below 250 psi. The LUVs containing DPX were more difficult to prepare than LUVs with ANTS. In general, more than 10 extrusions through 0.1 μm filters were required to yield LUVs with an absorbance at 700 nm of <0.250. Using our lipid compositions, we were not able to prepare LUVs in solutions containing 90 mM DPX, whereas phosphatidylserine LUVs were made in solutions containing 90 mM DPX (*20*). We were able to prepare LUVs with 50 mM DPX. Thus, we used $LUV^{12.5ANTS/25DPX}$ for leakage studies and LUV^{25ANTS} with LUV^{50DPX} for contents mixing studies.

To study Ca^{2+} effects, $CaCl_2$ solution (500 mM) was added to some of the LUV samples immediately before fluorescence measurements. The final concentration of Ca^{2+} in samples was 5 mM.

For samples at pH 6, LUV samples at pH 9 were dialyzed quickly (for 45 min) against 30 mM 2-(*N*-morpholino)-ethanesulfonic acid (MES) buffer (pH 6) containing 0.2 mM EDTA and 140 mM KCl with an osmolality of ~270 mmol/kg. Alternatively, 1 M MES with EDTA and KCl buffer at pH 6 was injected into LUV samples at pH 9 to give LUVs at pH 6 in 33 mM MES buffer. These two methods appeared to produce samples with very similar results in leakage and contents mixing assays. For example, mean values for the contents mixing assay at $t = 4.5$ h were $16.3 \pm 4.1\%$ for samples obtained with the dialysis method and $22.0 \pm 3.3\%$ for samples obtained with the injection method. Values for the content leakage assay at $t = 4.5$ h were $12.0 \pm 4.6\%$ for samples obtained with dialysis and $7.9 \pm 2.4\%$ for samples obtained with the injection method. Most of the data were collected on dialyzed LUVs.

Usually, under each experimental condition, three sets of samples were prepared for fluorescence intensity measurements.

Analysis of Lipid Composition, Lipid Concentration, and Vesicle Size. Lipid compositions in LUV-N^{25ANTS}, -X^{25ANTS}, and -Z^{25ANTS} were checked by high-performance thin-layer chromatography (*18*).

The cholesterol concentration in all LUV samples was determined by the cholesterol oxidase assay (*21*). A calibration curve was generated using cholesterol samples with known concentrations (1−50 μg/mL solutions), with and without cholesterol sulfate. We found that cholesterol sulfate did not interfere with the cholesterol oxidase assay. Values of cholesterol concentrations in samples were then used to calculate total lipid concentrations in samples.

Effective diameters of LUV-N, with and without ANTS/DPX, and their polydispersity values were determined by quasi-elastic light scattering measurements with cumulant analysis (*18*).

Fluorescence Intensity Measurements for Content Leakage and Contents Mixing Assays. A Hitachi F2000 fluorescence spectrophotometer (Tokyo, Japan) equipped with a circulating water bath set at 25 °C was used to measure fluorescence intensities of samples (~1.5 mL at a lipid concentration of ~1 mg/mL) in cuvettes whose contents were being stirred. The excitation was set at 384 nm, and the emission was detected at 540 nm. A Corning 3-69 cutoff filter was used to reduce light scattering effects (*10*). The beam shutter was activated between measurements to help reduce the amount of photobleaching in samples. Samples were stored in the dark until they were used.

The fluorescence intensities of ANTS in various types of LUVs with and without DPX were measured as a function of time (I_t), with I_0 taken at $t = 0$. The maximum (total) intensities of ANTS in all LUV samples (I^T) were measured in the presence of 0.5% (by volume) Triton X-100. For quenching experiments, I_0/I^T values were determined in samples of LUV-$N^{12.5ANTS/12.5DPX}$, LUV-$N^{12.5ANTS/25DPX}$, and LUV-$N^{12.5ANTS/45DPX}$ and in samples of DPPC $LUV^{12.5ANTS/12.5DPX}$, DPPC $LUV^{12.5ANTS/25DPX}$, and DPPC $LUV^{12.5ANTS/45DPX}$. Stern−Volmer plots (*22*) of I_0/I^T versus DPX concentrations were obtained.

The quenching of ANTS fluorescence in one LUV population by DPX in another LUV population is a measure of the extent of aqueous contents intermixing (*10*, *20*). Quenching by DPX is highly concentration-dependent, so release of contents from the vesicles and their dilution in aqueous space do not result in quenching (*20*). The aqueous contents of ANTS vesicles must mix with the aqueous contents of DPX vesicles to generate the distance-dependent energy transfer required for quenching. For contents mixing experiments, I_t values of samples containing equal volumes of LUV^{25ANTS} and LUV^{50DPX} were measured as a function of time, up to 5 h. Contents mixing (percent) values were calculated as $(I_0 - I_t)/I_0$.

The rate of release of contents from vesicles (leakage) was measured separately by co-encapsulating ANTS and DPX in one population of vesicles and measuring the increase in ANTS fluorescence as the probes (ANTS) leak from the vesicles to the medium. ANTS becomes diluted into the medium (*10*, *20*). ANTS does not self-quench since there is no overlap between its excitation and emission spectra (*10*). ANTS fluorescence is efficiently quenched by DPX by the classical Förster energy transfer mechanism and depends on the average distance between ANTS and DPX molecules (*10*). For content leakage experiments, I_0 and I_t (up to 5 h) of $LUV^{12.5ANTS/25DPX}$ samples were measured. Content leakage (percent) values were calculated as $(I_t - I_0)/(I^T - I_0)$.

Data were plotted with commercially available software (Origin from Microcal Software, Inc., Northampton, MA). Since data for our different runs, under the same experimental conditions, were not always obtained with same time points, each set of data was fitted by a spline function to give the best fit. Values at specific times were then calculated from fitted functions for each experimental run, and these values were averaged to give mean values and standard deviations. Thus, under each experimental condition, raw data from several, generally three, runs were reduced to one set of mean values, with standard deviations. These mean values under one experimental condition were used for comparison with those under another experimental condition.

RESULTS

Characterization of LUVs. Thin-layer chromatography data showed that the inclusion of fluorescent probe ANTS and/or cationic quencher DPX in lipid solutions did not affect the extrusion and column separation processes used in LUV preparation, and the lipid compositions of LUV-N, LUV-X, and LUV-Z, summarized in Table 1, remained the same as their starting compositions.

Mean effective diameters from dynamic light scattering measurements were 124 ± 9 nm, with a mean polydispersity of 0.114 ± 0.019 ($n = 2$) for LUV-N at pH 9. These values were similar to those published earlier, at lower osmolality values (*18*). Thus, increasing the buffer osmolality did not appear to change the mean effective diameter of LUVs. Mean effective diameters of LUV-$N^{12.5ANTS/25DPX}$ (used for content leakage studies), LUV^{25ANTS}, and LUV^{50DPX} (used for contents mixing studies) were also similar (Table 1). It has been reported that phospholipid vesicles increase in size with increasing cholesterol content, even when made by the same process (*11*). However, for our LUV systems with various cholesterol contents (15, 25, or 30% of total lipid content

Table 1: Cholesterol Sulfate and Cholesterol Compositions[a] (Weight %) and Effective Diameter of LUV-N, LUV-X, and LUV-Z

LUV type	cholesterol sulfate (%)	cholesterol (%)	ANTS[b] (mM)	DPX[b] (mM)	effective diameter (nm)[c]	PD[d]
LUV-N[c]	5	25	12.5	25	117 ± 20 (3)	0.102 ± 0.035
			25	−	116 ± 3 (3)	0.100 ± 0.022
			−	50	121 ± 14 (2)	0.145 ± 0.008
LUV-X[d]	15	15	12.5	25	111 ± 6 (4)	0.102 ± 0.035
			25	−	105 ± 9 (2)	0.088 ± 0.008
			−	50	121 ± 7 (2)	0.137 ± 0.064
LUV-Z	0	30	12.5	25	124 ± 9 (3)	0.118 ± 0.043
			25	−	119 ± 35 (2)	0.164 ± 0.064
			−	50	154 ± 16 (3)	0.181 ± 0.076

[a] The remaining lipid compositions consisted of 55% ceramides (composed of a 3:2 weight ratio of bovine brain ceramides type III and IV, respectively) and 15% fatty acids [1:2:1 (by weight) palmitic acid:lignoceric acid:octacosanoic acid]. [b] The concentrations listed were the concentrations in solutions used to make LUVs. The concentrations of ANTS and DPX inside LUVs were not determined. [c] Average effective diameter in nanometers of LUVs measured by quasi-elastic light scattering methods ± SD (n = the number of different samples used). [d] PD is polydispersity (the relative width of the distribution of effective diameters).

for LUV-X, LUV-N, or LUV-Z, respectively), similar effective diameters (about 120 nm) were obtained (Table 1). Most of the polydispersity values were around or less than 0.150, suggesting that the LUV effective diameters were narrowly distributed. The polydispersity values of two systems (LUV-Z^{25ANTS} and LUV-Z^{50DPX}) were >0.150, but <0.185, suggesting a slightly broader distribution of sizes in these two systems.

Binding of ANTS to LUVs. The mean intensity of LUV-N incubated with 25 mM ANTS followed by column chromatography to remove unbound ANTS was 33.0 ± 0.3 (n = 3), and the fluorescence intensity for plain LUV-N was 27.9 ± 0.04. The difference of 5.1 was considered to be the fluorescence intensity of ANTS bound to LUV-N. The mean fluorescence intensity of LUV-N^{25ANTS} was 457 ± 121 (n = 3). Thus, bound ANTS contributed about 1.1% of the total fluorescence intensity of LUV-N^{25ANTS}. Similar values were obtained for DPPC $LUV^{12.5ANTS}$. Our findings of little ANTS binding to stratum corneum vesicles were similar to the published results on phospholipid vesicles (*20*).

DPX Quenching. Since we were unable to prepare LUVs with 90 mM DPX, as required in the published protocol for phospholipid vesicles (*10*, *20*), we decreased the concentrations of DPX in buffers to 12.5, 25, or 50 mM and ANTS concentrations in vesicle preparation buffers at pH 9 to 12.5 mM. We followed the DPX quenching in both stratum corneum LUV-N and DPPC LUV systems at pH 9. In general, the excited ANTS collides with DPX to form an excited-state encounter complex which undergoes an internal fluorescence quenching reaction. This is dynamic quenching and is represented by a linear Stern−Volmer plot. When the quencher forms a ground-state ANTS complex, it undergoes static quenching. The total degree of quenching is thus a product of the dynamic and static terms with an upward curving Stern−Volmer plot (*22*). This upward curving behavior is commonly observed for efficient quenchers. Both stratum corneum LUV-N and DPPC LUV systems exhibited upward curving Stern−Volmer plots (Figure 1), suggesting that 25 mM DPX in $LUV^{12.5ANTS25DPX}$ was an efficient quencher at pH 9. ANTS/DPX leakage assays have also been used previously at pH 9.5 on phospholipid vesicles (*23*). Measurements of quenching efficiency at pH 6 were not taken, but since ANTS fluorescence is relatively independent of pH between 4.0 and 7.5 (*10*), we assumed a similar quenching efficiency at pH 6.

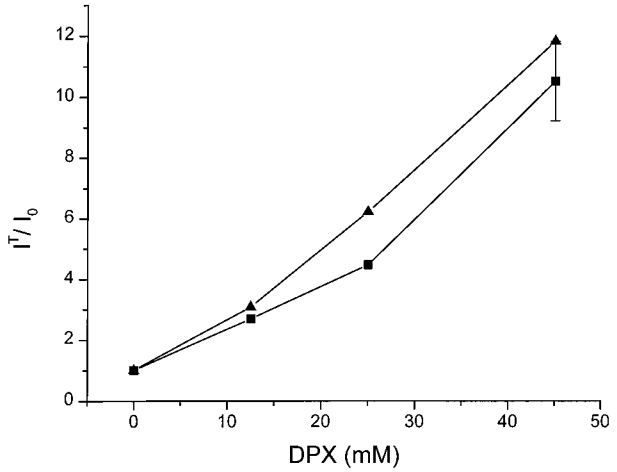

FIGURE 1: Stern−Volmer plot. Quenching of ANTS by DPX in LUV samples prepared with buffers (pH 9) containing 12.5 mM ANTS and various amounts of DPX, as indicated on the x-axis. Fluorescent intensities of these LUV samples taken at t = 0 (I_0) and their maximum intensities in the presence of 0.5% (by volume) Triton X-100 (I^T) were measured. The squares (■) represent data for stratum corneum LUV-N (see Table 1 for lipid composition), and the triangles (▲) represent data for DPPC LUVs. The values for quenching in these two systems were very similar. The data points exhibited an upward curvature, suggesting that the quenching was a product of both dynamic and static terms. This upward curvature behavior is commonly observed for efficient quenchers. For content leakage assays, we used LUVs prepared with 12.5 mM ANTS and 25 mM DPX.

Aqueous Contents Mixing. Little contents mixing was observed for all three LUV systems at pH 9 (Figure 2, bottom). The mean values obtained at t = 5 h were 4.1% for LUV-N, 1.8% for LUV-X, and 5.6% for LUV-Z, with a standard deviation of about 3%. The addition of 5 mM $CaCl_2$ to these LUV systems induced rapid contents mixing, with about 30% contents mixing within the first 3 min of measurement for all three LUV systems (Figure 2, top). The contents mixing processes appeared to level off at about t = 1 h, with the values being 35.9% for LUV-N, 33.6% for LUV-X, and 36.2% for LUV-Z. At t = 5 h, the values remained similar (35.9% for LUV-N, 34.3% for LUV-X, and 37.0% for LUV-Z, with a standard deviation of about 3%).

Changing the sample pH from pH 9 to 6 by dialysis induced contents mixing (Figure 2, middle). At t = 5 h, the values increased to 16.4% for LUV-N, 10.6% for LUV-X,

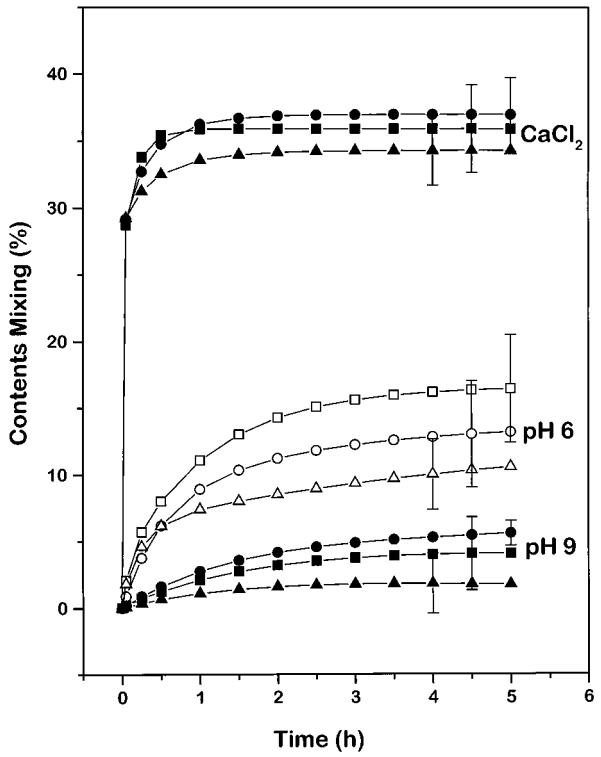

FIGURE 2: Aqueous contents mixing of LUVs. Squares (■) represent mean values of data for LUV-N, triangles (▲) for LUV-X, and circles (●) for LUV-Z. See Table 1 for lipid compositions of these LUV samples. The LUVs were prepared in buffers containing 25 mM ANTS (LUV^{25ANTS}) and in buffers containing 50 mM DPX (LUV^{50DPX}). The concentrations of ANTS and DPX inside LUVs were not determined. The maximum fluorescence intensities of ANTS (I^T) in each LUV sample were measured by adding 0.5% (by volume) Triton X-100 to the LUV system. Florescence intensities of samples containing equal volumes of LUV^{25ANTS} and LUV^{50DPX} were measured as a function of time (I_t), up to 5 h. Contents mixing (percent) values were calculated as $(I_0 - I_t)/I_0$, where I_0 was measured at $t = 0$. LUVs were prepared at pH 9. $CaCl_2$ solutions (500 mM) were added to LUV samples immediately before fluorescence measurements were taken to give a final concentration of 5 mM. For samples at pH 6, LUV samples at pH 9 were dialyzed quickly (for 45 min) against 30 mM MES buffer at pH 6. Three or four runs were carried out under each condition. The standard deviations ranged from 3 to 4%.

and 13.2% for LUV-Z, with standard deviations of about 4%.

Content Leakage. At pH 9, little content leakage was detected for all three types of LUV samples ($LUV\text{-}N^{12.5ANTS/25DPX}$, $LUV\text{-}X^{12.5ANTS/25DPX}$, and $LUV\text{-}Z^{12.5ANTS/25DPX}$) up to 5 h after the vesicles were prepared (Figure 3, bottom). The values obtained from content leakage assays were all around baseline. The addition of $CaCl_2$ (5 mM) drastically increased the degree of content leakage for all three systems (Figure 3, top). At $t = {}^1/_2$ h, about 18% content leakage was detected for LUV-N and LUV-X whereas about 13% leakage was detected for LUV-Z. At $t = 5$ h, the degree of leakage leveled off to about 30% for both LUV-N and LUV-X, whereas the degree of content leakage continued to increase to about 45% for LUV-Z.

Content leakage was detected at pH 6, however to a lesser extent than that induced by 5 mM $CaCl_2$ (Figure 3, middle). Leakage began immediately, with about 6−10% content leakage detected during the first hour of monitoring for LUV-N and LUV-X. For LUV-Z, however, content leakage

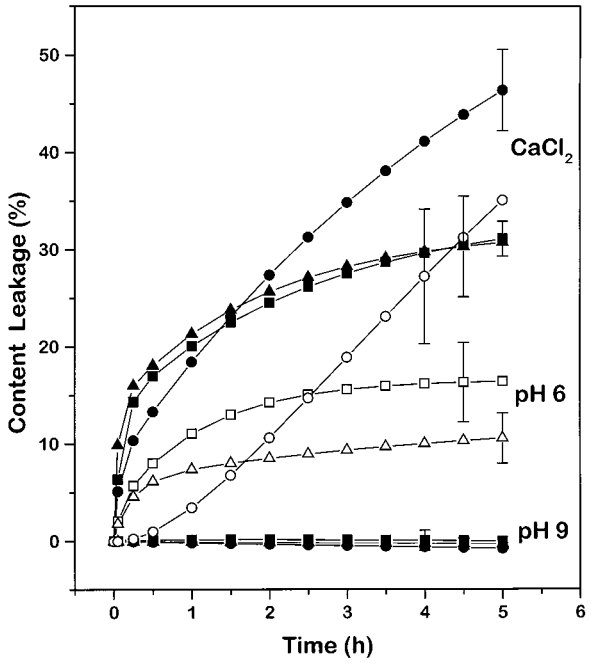

FIGURE 3: Contents leakage assay of LUVs. Squares (■) represent the mean values of data for LUV-N, triangles (▲) for LUV-X, and circles (●) for LUV-Z. See Table 1 for lipid compositions of these LUV samples. The LUVs were prepared in buffers containing 12.5 mM ANTS and 25 mM DPX. The concentrations of ANTS and DPX inside LUVs were not determined. Florescence intensities as a function of time (I_t) were measured up to 5 h. The maximum fluorescence intensities (I^T) were measured by adding 0.5% (by volume) Triton X-100. Content leakage (percent) values were calculated as $(I_t - I_0)/(I^T - I_0)$, where I_0 was measured at $t = 0$. LUVs were prepared at pH 9. $CaCl_2$ solutions (500 mM) were added to LUV samples immediately before fluorescence measurements were taken to give final $CaCl_2$ concentrations of 5 mM. For samples at pH 6, LUV samples at pH 9 were dialyzed quickly (for 45 min) against 30 mM MES buffer at pH 6. Three or four runs were carried out under each condition.

was delayed. Approximately 1% content leakage was detected for LUV-Z at $t = {}^1/_2$ h, and the degree of leakage reached a level of ∼3% after 1 h. The content leakage continued beyond the first hour for all three systems, and at $t = 5$ h, the degree of content leakage appeared to level off to about 16% for LUV-N and 11% for LUV-X, but continued to increase to 35% for LUV-Z.

DISCUSSION

In this study, the effects of calcium and pH on vesicle leakage and aqueous contents mixing were studied on stratum corneum lipid LUVs containing three different cholesterol: cholesterol sulfate ratios to better understand stratum corneum lipid interactions and the effect of cholesterol sulfate. Most stratum corneum lipid studies have been carried out on small unilamellar vesicle (SUV) systems. For example, morphological changes in stratum corneum lipid assembly upon addition of corneocytes (*24*), salt (*24*), acylceramides and acylglucosylceramides (*25*, *26*), and calcium (*27*) were observed in SUV systems. SUVs prepared with either no free fatty acids or no cholesterol sulfate were used to study calcium effects on stratum corneum lipids (*27*). However, lipid molecules in SUVs experience unusual molecular packing in their bilayer due to their high level of curvature (*28*). The higher percentage (60−70%) of lipids in the outer

monolayer of SUV compared to the inner monolayer can lead to asymmetric distribution of lipids in vesicles (*29*). Asymmetric lipid distribution may affect lipid−lipid and/or lipid−protein interactions. Thus, it may be difficult to relate experimental results to functional properties in SUV studies. Stratum corneum LUVs are relatively more stable and may better serve as a model system for understanding lipid interactions in stratum corneum with different lipid compositions.

Contents mixing and content leakage assays are two methods widely used to study intervesicle lipid interactions (*23*, *30*, *31*). It has been shown that lipid vesicles interact to yield fusion, lysis, and/or mixing of bilayer components (*20*). For the first case, fusion is defined as the concomitant mixing of bilayer lipids and aqueous contents. For the second case, lysis involves no mixing of aqueous contents, but leakage and mixing of bilayer lipids. The third case may be due only to outer monolayer mixing while the inner monolayer remains intact (*20*). The lipid interactions leading to vesicle fusion may be observed with a contents mixing assay, and the lipid interactions leading to vesicle lysis may be observed with a content leakage assay. We modified the published contents mixing and content leakage assays, which were developed for phospholipid systems, for stratum corneum lipid systems, and used them to evaluate intervesicle lipid interactions in LUVs with various stratum corneum lipid compositions. Since different assays follow different kinetic or equilibrium properties in lipid interactions, each assay monitors slightly different molecular events (*20*, *32*). Therefore, these two assays provide complementary information on vesicle lipid interactions. It has been shown that the ANTS/DPX assay monitors a faster fusion event than the terbium/dipicolinate assay (*20*, *33*). It has also been reported that the contents mixing assay is very sensitive to lipid aggregation (*32*). In addition, small changes in the average size of the liposomes led to significant changes in the fusion kinetics (*20*, *34*). In our studies, we focused on comparing the relative extent of intervesicle lipid interactions in our LUV systems with three different lipid compositions, rather than the absolute values for vesicle fusion or for vesicle lysis.

Results from both contents mixing and content leakage assays indicated little intervesicle lipid interactions at pH 9 in all three types of LUVs studied. At pH 9 and room temperature, LUV-X (15% cholesterol sulfate) and LUV-Z (no cholesterol sulfate) samples exhibited stabilities similar to that of LUV-N (5% cholesterol sulfate) samples. Earlier, we have shown that LUV-N samples remain in solution, and are free of lipid aggregation for 4−6 weeks at room temperature (*18*).

In this study, we found that, at pH 9, the addition of Ca^{2+} (5 mM) to LUVs activated intervesicle lipid mixing, leading to both contents mixing and content leakage in all three types of LUVs. About 30−40% LUVs exhibited contents mixing (fusion) within 30 min of addition of Ca^{2+} in all three stratum corneum LUV systems. However, for the Ca^{2+}-induced content leakage (lysis), differences were observed between systems with and without cholesterol sulfate. For LUV-N and LUV-X systems, Ca^{2+}-induced interactions led to 20% content leakage/vesicle lysis within 1 h, and leveled off to about 25% at 5 h. For the LUV-Z system, however, content leakage was initially slower than that for LUV-N and LUV-X systems, but was followed by more rapid leakage after 1.5 h. After 5 h, about 50% of the vesicles exhibited leakage, and the degree of leakage did not appear to level off. The increased extent of Ca^{2+}-induced leakage for vesicles without cholesterol sulfate suggests that Ca^{2+} binds to the fatty acid's carboxylate group at the surface of the LUVs, leading to the collapse of LUV-Z vesicles, presumably into other structures, whereas the vesicles with cholesterol sulfate (LUV-N and LUV-X) remain relatively stable due to cholesterol sulfate's contribution to the surface charge of the vesicles. Thus, the extent of calcium-induced leakage for vesicles containing both fatty acids and cholesterol sulfate was less than the extent of massive leakage observed in vesicles without cholesterol sulfate. Previous EM studies showed that SUVs without cholesterol sulfate began to fuse to form larger vesicles and lamellar sheet within 1 h of the addition of Ca^{2+}, and only lamellar sheet structures were found after 2 weeks (*27*). The SUVs with cholesterol sulfate and fatty acids remained as larger vesicles with only some lamellar sheets, and the SUVs with cholesterol sulfate but no fatty acid did not fuse after 2 weeks (*27*).

The physiological relevance of Ca^{2+} to stratum corneum formation has been previously suggested (*27*, *36*). Menon and co-workers used ion capture chromatography to show high levels of extracellular Ca^{2+} present at the stratum granulosum−stratum corneum interface. Lamellar granules are thought to discharge their contents into intercellular space as flattened unilamellar vesicles (*37*). The high Ca^{2+} levels at the interface might activate the fusion of unilamellar vesicles into broad lipid lamellar sheets, which form the stratum corneum (*27*). Recently, Elias and co-workers demonstrated the importance of a calcium gradient in barrier formation. In rodent epidermis, a calcium gradient forms at the same time as the stratum corneum barrier competence is established (*38*). The gradient exhibits low levels of Ca^{2+} in the stratum corneum and higher levels of Ca^{2+} at the stratum corneum−stratum granulosum interface. In agreement with this finding, our results showed that Ca^{2+} promoted lipid interactions in all vesicle systems studied. We did not observe differences in Ca^{2+}-induced fusion between vesicles with a high cholesterol sulfate content (LUV-X) and vesicles with 5% cholesterol sulfate (LUV-N). In recessive X-linked ichthyosis, significantly higher cholesterol sulfate levels are only present at the stratum corneum layer (*19*). Since the Ca^{2+} concentration is low in the stratum corneum, lack of differences in Ca^{2+}-induced lipid interactions between vesicles modeled with ichthyosis and normal lipid compositions might not be surprising.

Lower levels of cholesterol sulfate are present in the upper layer of the stratum corneum than in entire stratum corneum sheets (*39*). Some cholesterol sulfate is needed to prevent collapse of all vesicle structures prior to final stratum corneum bilayer formation. Too much cholesterol sulfate present, i.e., ∼15 wt % as in the case for recessive X-linked ichthyosis, along with decreased levels of cholesterol might prevent proper extended bilayer formations in the uppermost layer of the stratum corneum. The rate of intermembrane exchange for cholesterol sulfate was found to be approximately 10-fold faster than for cholesterol (*11*). Thus, it is possible that intervesicle lipid interactions may lead to rapid exchange of cholesterol sulfate between bilayers.

A decrease in pH to pH 6, the pH of the skin (*40*, *41*), also activated intervesicle lipid mixing, but to a lesser extent

than that activated by Ca^{2+}. The overall extents of vesicle fusion (contents mixing) and vesicle lysis (content leakage) at pH 6 were about 10% in LUV-N and LUV-X systems. LUV-Z exhibited continuous vesicle lysis at pH 6, as in the case for LUV-Z with 5 mM Ca^{2+}. Proton-induced vesicle fusion and lysis in phospholipid systems have also been reported (*10*, *20*, *42*). The activation of lipid mixing of LUVs at pH 6 but not at pH 9 may again be due to the neutralization of the fatty acid carboxylate group at the surface of the vesicles, as has been speculated for the fusion of phosphatidylethanolamine/oleic acid vesicles at pH 6 (*42*). It has been suggested that neutralization of fatty acids allows vesicles to closely approach each other. Free fatty acids within lipid membranes exhibit much higher pK_a values, ~6−8 (*43*−*45*), than the fatty acids in aqueous solution. The pK_a values in aqueous solution are about 4.8 (*46*). The shift of about 1.5−3 pK_a units when a fatty acid is intercalated in a bilayer reflects the effects of a low dielectric constant at the water−hydrocarbon chain interface, specific fatty acid headgroup interactions, associated water, surface charge, and ionic strength on fatty acid ionization (*47*). The pK_a values for fatty acids on stratum corneum model lipid membranes were between 6 and 7.3, depending on the lipid composition and temperature (*45*, *47*). The effect of cholesterol sulfate on fatty acid ionization in stratum corneum model lipid membranes has also been studied, and the inclusion of 5% cholesterol sulfate results in a 0.3 pK_a unit increase (*47*). In the same study, Wiedmann et al. found multiple fatty acid environments below pH 7 when cholesterol sulfate was excluded from the composition. Since the apparent pK_a of fatty acids in stratum corneum membranes is between 6 and 7.3, a large percentage of fatty acids would be neutralized at pH 6. In our previous studies of LUV-N at pH 6, we have observed increases in the LUV effective diameter and polydispersity as a function of time, accompanied by the eventual precipitation of lipid (*18*). Furthermore, as cholesterol sulfate was found to increase the pK_a of the fatty acids, a higher level of neutralization would be present in vesicles free of cholesterol sulfate. The lack of additional charge stabilization of the bilayer and an increase in the pK_a of fatty acids when cholesterol sulfate is absent are most likely responsible for the increased degree of lysis found in LUV-Z systems.

Our results showed that higher levels of cholesterol sulfate in the LUV-X vesicles did not prevent fusion or leakage at pH 6. Although cholesterol sulfate contributes a greater surface charge to the vesicles and might be expected to reduce the extent of fusion, the amount of cholesterol sulfate in our LUV systems was increased at the expense of cholesterol. The stabilizing effect of cholesterol on bilayer formation would be compromised with an increase in the level of cholesterol sulfate.

Elias and co-workers found that acidic pH initiates barrier recovery (*48*). Our pH results supported this finding. Little intervesicle lipid interaction is present at pH 9, regardless of lipid composition, and reduction to pH 6 initiates fusion and lysis with eventual formation of lamellar sheets. pH-dependent alterations in barrier recovery were also found to be independent of Ca^{2+}-controlled secretion of lamellar disks (*48*).

In conclusion, our results suggested that fusogenic agents such as Ca^{2+} and H^+ act to neutralize the fatty acids in the lipid bilayer of stratum corneum vesicles. The inclusion of 5−15% cholesterol sulfate helps to prevent the collapse of fused vesicles into other structures.

REFERENCES

1. Gray, G. M., White, R. J., Williams, R. H., and Yardley, H. J. (1982) *Br. J. Dermatol. 106*, 59−63.
2. Wertz, P. W., Swartzendruber, D. C., Madison, K. C., and Downing, D. T. (1987) *J. Invest. Dermatol. 89*, 419−425.
3. Elias, P. M., and Friend, D. (1975) *J. Cell Biol. 65*, 180−191.
4. Madison, K. C., Swartzendruber, D. C., Wertz, P. W., and Downing, D. T. (1987) *J. Invest. Dermatol. 88*, 714−718.
5. Brysk, M. M., and Rajaraman, S. (1992) *Prog. Histochem. Cytochem. 25*, 1−53.
6. Williams, M. L. (1992) *Semin. Dermatol. 11*, 169−175.
7. Koppe, J. G., Marinkovic-Iisen, A., Rijken, Y., de Groot, W. P., and Jobsis, A. C. (1978) *Arch. Dis. Child. 53*, 803−806.
8. Sharpiro, L. J., Weiss, R., Webster, D., and France, J. T. (1978) *Lancet 1*, 70−72.
9. Williams, M. L., and Elias, P. M. (1981) *J. Clin. Invest. 68*, 1404−1410.
10. Ellens, H., Bentz, J., and Szoka, F. C. (1984) *Biochemistry 23*, 1532−1538.
11. Rodrigueza, W. V., Wheeler, J. J., Klimuk, S. K., Kitson, C. N., and Hope, M. J. (1995) *Biochemistry 34*, 6208−6217.
12. Mao-Qiang, M., Feingold, K. R., and Elias, P. M. (1993) *Arch. Dermatol. 129*, 728−738.
13. Zettersten, E. M., Ghadially, R., Feingold, K. R., Crumrine, D., and Elias, P. M. (1997) *J. Am. Acad. Dermatol. 37*, 403−408.
14. Schmid, M. H., and Korting, H. C. (1994) *Crit. Rev. Ther. Drug Carrier Syst. 11*, 97−118.
15. Lampe, M. A., Burlingame, A. L., Whitney, J., Williams, M. L., Brown, B. E., Roitman, E., and Elias, P. M. (1983) *J. Lipid Res. 24*, 120−130.
16. Wertz, P. W., Abraham, W., Landmann, L., and Downing, D. T. (1986) *J. Invest. Dermatol. 87*, 582−584.
17. Abraham, W. (1992) *Semin. Dermatol. 11*, 121−128.
18. Hatfield, R. M., and Fung, L. W.-M. (1995) *Biophys. J. 68*, 196−207.
19. Elias, P. M., Williams, M. L., Maloney, M. E., Bonifas, J. A., Brown, B. E., Grayson, S., and Epstein, E. H., Jr. (1984) *J. Clin. Invest. 74*, 1414−1421.
20. Ellens, H., Bentz, J., and Szoka, F. C. (1985) *Biochemistry 24*, 3099−3106.
21. Barenholz, Y., Patzer, E. J., Moore, N. F., and Wagner, R. R. (1978) *Adv. Exp. Med. Biol. 101*, 45−56.
22. Eftink, M. R. (1991) in *Topics in Fluorescence Spectroscopy* (Lakowicz, J. R., Ed.) Vol. 2, p 53, Plenum Press, New York.
23. Bennett, D. E., and O'Brien, D. F. (1995) *Biochemistry 34*, 3102−3113.
24. Abraham, W., and Downing, D. (1990) *Biochim. Biophys. Acta 1021*, 119−125.
25. Abraham, W., Wertz, P. W., and Downing, D. T. (1988) *Biochim. Biophys. Acta 939*, 402−408.
26. Abraham, W., Wertz, P. W., and Downing, D. T. (1988) *J. Invest. Dermatol. 90*, 259−262.
27. Abraham, W., Wertz, P. W., Landmann, L., and Downing, D. T. (1987) *J. Invest. Dermatol. 88*, 212−214.
28. Lawaczeck, R., Kainosho, M., and Chan, S. I. (1976) *Biochim. Biophys. Acta 443*, 313−330.
29. Szoka, F., and Papahadjopoulos, D. (1980) *Annu. Rev. Biophys. Bioeng. 9*, 467−508.
30. Lee, J. K., and Lentz, B. R. (1997) *Biochemistry 36*, 421−431.
31. Franzin, C. M., and Macdonald, P. M. (1997) *Biochemistry 36*, 2360−2370.
32. Düzgünes, N. T., Allen, M., Fedor, J., and Papahadjopoulos, D. (1987) *Biochemistry 26*, 8435−8442.
33. Wilschut, J., Düzgünes, N., and Papahadjopoulos, D. (1981) *Biochemistry 20*, 3126−3133.
34. Lentz, B. R., McIntyre, G. F., Parks, D. J., Yates, J. C., and Massenburg, D. (1992) *Biochemistry 31*, 2643−2653.

35. Bentz, J., Düzgünes, N., and Nir, S. (1985) *Biochemistry 24*, 1064−1072.
36. Menon, G. K., Grayson, S., and Elias, P. M. (1985) *J. Invest. Dermatol. 84*, 508−512.
37. Landmann, L. (1984) *Eur. J. Cell Biol. 33*, 258−264.
38. Elias, P. M., Nau, P., Hanley, K., Cullander, C., Crumrine, D., Bench, G., Sideras-Haddad, E., Mauro, T., Williams, M., and Feingold, K. R. (1998) *J. Invest. Dermatol. 110*, 399−404.
39. Ranasinghe, A. W., Wertz, P. W., Downing, D. T., et al. (1986) *J. Invest. Dermatol. 86*, 187−190.
40. Behrendt, H., and Green, M. (1971) *Patterns of Skin pH from Birth through Adolescence*, Charles C. Thomas, Springfield, IL.
41. Braun-Falco, O., and Korting, H. (1986) *Hautarzt 37*, 126−129.
42. Düzgünes, N., Staubinger, R. M., Baldwin, P. A., Friend, D. S., and Papahadjopoulos, D. (1985) *Biochemistry 24*, 3091−3098.
43. Ptak, M., Egret-Charlier, M., Sanson, A., and Bouloussa, O. (1980) *Biochim. Biophys. Acta 600*, 387−397.
44. Krämer, S. D., Jakits-Deiser, C., and Wunderli-Allenspach, H. (1997) *Pharm. Res. 14*, 827−832.
45. Lieckfeldt, R., Villalían, J., Gómez-Fernández, J.-C., and Lee, G. (1995) *Pharm. Res. 12*, 1614−1617.
46. Spector, A. (1975) *J. Lipid Res. 16*, 165−179.
47. Wiedmann, T. S., Hamilton, J. T., and Salmon, A. (1995) *Proc. Int. Symp. Controlled Release Bioact. Mater., 22nd, 1995*, 716−717.
48. Mauro, T., Grayson, S., Gao, W. N., Man, M.-Q., Kriehuber, E., Behne, M., Feingold, K., and Elias, P. M. (1998) *Arch. Dermatol. Res. 290* (4), 215−222.

BI981421K